Journal of Theoretical and Applied Information Technology
15th October 2021. Vol.99. No 19

ISSN: 1992-8645 www.jatit.org E-ISSN: 1817-3195

STEADY STATE ANALYSIS OF DYNAFLOW CONTROLLER

[1]RAGALEELA DALAPATI RAO, [2]PADMANABHA RAJU CHINDA

[1,2] Department of Electrical and Electronics Engineering, Prasad V. Potluri Siddhartha Institute of Technology, Vijayawada, India

E-mail: [1]raga_233@yahoo.co.in, [2]pnraju78@yahoo.com ,

ABSTRACT

A new member in flexible ac transmission systems (FACTS) known as dynaflow controller is presented in this paper. It is being used to regulate the flow of power in electrical transmission networks. Dynaflow controller can provide both series and shunt compensation, so, it can be called as hybrid compensator. It basically consists of a thyristor controlled phase shifting transformer (TCPST) and thyristor switched series capacitor (TSSC). This paper presents the equivalent circuit, the load flow model and the simple linear operation of the dynaflow controller. The newton-raphson power flow integrates the Dynaflow controller design and assesses various network parameters. The device's efficiency is evaluated on the conventional IEEE 30 bus system and the load flow analysis results are reported.

Keywords: *Flexible AC Transmission System (FACTS); Dynaflow Controller; Thyristor Controlled Phase Shifting Transformer (TCPST); Thyristor Switched Series Capacitor (TSSC); power flow analysis*

1. INTRODUCTION

Increased demand and network ageing make that power flow in power transmission systems can indeed be controlled quickly and reliably [1]. The flexible ac-transmission (FACTS) system is defined by the IEEE as "a power-electronic system and other static systems that control one or more ac-transmission system parameters for increased control and energy transfer" [2], and can be used for power-flow control. FACTS's idea is to make existing power system capabilities more controllable and optimized using reliable high-speed electronics instead of mechanical controls [3]. The possibility arises from FACTS devices' ability to control transmission systems parameters, which include series/shunt impedances, phase angle and oscillation damping at different frequencies under the rated frequency. Such restrictions cannot be overcome otherwise without reducing transmission capacity while maintaining the required system stability through mechanical means [4]. FACTS controllers can provide additional flexibility to allow a line to transport power closer to its ratings [5-10].

Study of simple linear power flow control is crucial in interlinked electricity grid operation. The study of different FACTS devices can be found in the technical literature [11 –13]. This article discusses the dynaflow controller as a new FACTS controller as well as discusses its steady state operating principle, a single line equivalent model and its power flow control qualities. Dynaflow controller is a blend of a phase shifting transformer (PST) and a thyristor switched series capacitor (TSSC) [14 –16]. TSSC present in the dynaflow controller is an electronically switched device. So, it can respond very fastly for system dynamics and its power flow control will be dynamic. In this paper only steady sate analysis of dynaflow controller is presented. Dynamic control of the dynaflow device was well investigated.

Dynaflow controller is a hybrid compensating device as it can control power flow in series and shunt compensation modes similar to unified power flow controller (UPFC). Dynaflow controller can be considered as an alternative device to UPFC. Dynaflow controller will be available at a lesser cost, simple and rugged design, easy to operate, lower losses and its efficiency is high. TSSC present in the dynaflow controller can be switched on and off by using thyristor switches. It was not phase controlled and as PST was included with TSSC, it will not produce any harmonics. So, the power quality will not be affected by this device.

Journal of Theoretical and Applied Information Technology
15th October 2021. Vol.99. No 19

ISSN: 1992-8645 www.jatit.org E-ISSN: 1817-3195

The literature survey shows that there are various FACTS devices can control many parameters of transmission lines, which a brief survey of these devices is presented as follows. Phase shifting transformer [15], UPFC [16], Thyristor Controlled Series Compensator (TCSC) [17], Static Var Compensator (SVC) [18], Static Synchronous Series Compensator (SSSC) [19, 20], Interline Power Flow Controller (IPFC), and Optimal Unified Power Flow Controller (OUPFC) [21], Static Synchronous Compensator (STATCOM) and so on.

Steady state single line identical layout of the dynaflow controller was presented in this paper. A power flow model was developed and technical features of the dynaflow device were tested on an IEEE 30 bus test system under various operating conditions, i.e. base load condition and contingency condition. A comparison between dynaflow controller with that of PST and TSSC are also presented.

The document that remains is divided into several sections. In Section 2, schematic configuration of Dynaflow and in Section 3 mathematical modeling of dynaflow controller is considered. The process for integrating dynaflow into the problem of load flow is seen in the Section 4. The results of the simulation are seen in Section 5 and, finally, in Section 6, the conclusions are drawn.

2. DYNAFLOW CONTROLLER SCHEMATIC CONFIGURATION

It combines TCPST and a TSSC, being in fact a hybrid device. In this study, a Dynaflow controller with a TCPST and a TSSC are considered. The Dynaflow controller, shown in Fig. 1, is a combination of TCPST [22] and TSSC that provides a set of thyristor-controlled capacitive reactivity steps connected to the line in series. Fig. 2 shows a single line configuration of the Dynaflow controller that is connected within the transmission line between busses m and n and consists of:

- Thyristor Controlled phase-shifting transformer (TCPST) that can inject lead/lag, quadrature-phase voltage

- In discrete steps, the TSSC can insert a variable series of capacitive reactivity to adjust the line series reactance. The relief of overload and operation in stressed situations are handled by the TSSC.

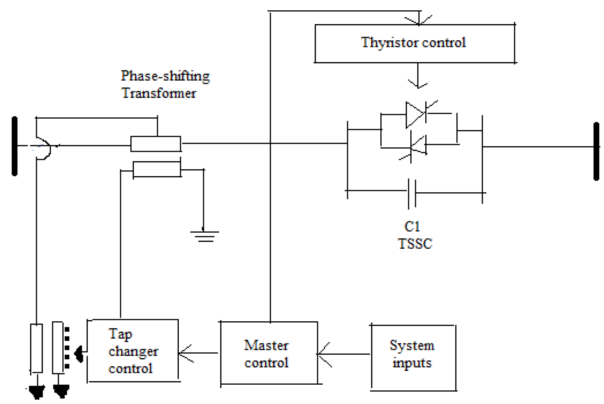

Fig. 1 Schematic Configuration Of Dynaflow Controller

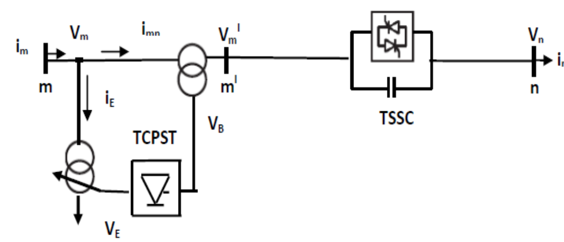

Fig. 2. Generic Image Of Dynaflow Device

In terms of power flow control and simplicity, this system is intended to be very efficient

3. GENERALIZED MATHEMATICAL MODELING OF DYNAFLOW CONTROLLER

It combines As mentioned in section 2, the dynaflow controller consists of 2 primary components. Fig. 2 shows a graphical dynaflow diagram that is related between buses m and n in a transmission system. V_B is an injected voltage in series and V_E is a PST voltage injected in parallel. From Fig. 2, the injected PST series voltage can be expressed as

$$V_B = jkV_E \tag{1}$$

In order to maximise power transfer, k is the PST voltage ratio (0<k<1). Because the ideal PST transformer of Fig. 2 does not interchange actual or reactive power.

$$V_B I_{mn}^* = V_E I_E^* \tag{2}$$

From Eq. (1) and (2), it is deduced as

$$I_E = -jkI_{mn} \tag{3}$$

Excitation voltage V_E is also given by

$$V_E = V_m - jX_E I_E \tag{4}$$

ISSN: 1992-8645 www.jatit.org E-ISSN: 1817-3195

Where, X_E is the leakage reactance of the excitation transformer (Fig. 2). Substituting for IE from Eq. (3) in Eq. (4) and then substituting for V_E in Eq. (1)

$$V_B = jkV_m - jk^2 X_E I_{mn} \tag{5}$$

Voltage $V_m^/$ is given by

$$V_m^/ = V_m + V_B - jI_{mn} X_B \tag{6}$$

Substituting V_B from Eq. (5) in Eq. (6) we get,

$$V_m^/ = (1+jk)V_m - j(k^2 X_E + X_B)I_{mn} \tag{7}$$

Where, X_B is the booster /series transformer leakage reactance. Voltage at terminal n can be calculated from the voltage at bus by subtracting the voltage drop of the TSSC module

$$V_n = V_m^/ + jk_C X_C I_{mn} \tag{8}$$

Where coefficient k_c determines the amount X_c of in service (ohmic losses are ignored).

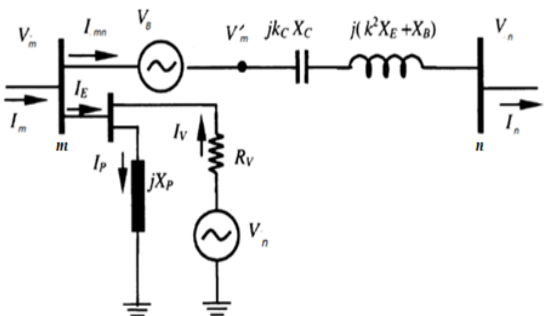

Fig. 3 Shows A Single Line Equivalent Model For Dynaflow With Two Independent Parameters Of Control:

i) PST voltage ratio (i.e.k)

ii) Series compensation level for impedance (i.e. k_c)

It should be noted that in Fig. 3, X_E, X_B, X_P and R_V are PST internal parameters. Where R_V is a resistive element and X_P is a capacitive element [23]. By substituting $V_m^/$ from Eq. (6) in Eq. (8), the line current is determined

$$I_{mn} = \frac{(1+jk)V_m}{jX_{mn}} - \frac{V_n}{jX_{mn}} \tag{9}$$

Where

$$X_{mn} = k^2 X_E + X_B - k_c X_c \tag{10}$$

At bus m, the injected current is

$$I_m = I_E + I_{mn} \tag{11}$$

Substituting for I_E and I_{mn} from equations (3) and (9) respectively in equation (11), then deduced as

$$I_m = (1+k^2)Y_{mn}V_m - (1-jk)Y_{mn}V_n \tag{12}$$

Where, $Y_{mn} = 1/jX_{mn}$

At bus n, we have

$I_n = I_{mn}$

Substituting for I_{mn} from equation (9) in equation (3), current of the excitation transformer of Fig. 2 can be reflected by

$$I_E = \frac{-k(1+jk)}{X_{mn}}V_m + \frac{k}{X_{mn}}V_n \tag{13}$$

From Fig. 3 I_E can be decomposed into two components I_P and I_V

$$I_E = I_P + I_V \tag{14}$$

Where

$$I_p = \frac{V_m}{j(\frac{X_{mn}}{k^2})} \; and \; I_v = \frac{V_n - V_m}{(\frac{X_{mn}}{k})} \tag{15}$$

Thus, equation (13) can be rewritten as

$$I_E = \frac{V_m}{jX_p} + \frac{V_n - V_m}{R_v} \tag{16}$$

Where

$$X_p = \frac{X_{mn}}{k^2}, \; R_v = kX_p \tag{17}$$

Dynaflow can actively adjust its internal parameters (i.e., PST (k) voltage ratio, series impedance compensation ($k_C X_C$). Therefore dynaflow regulates actual power flow and voltage magnitude. Dynaflow will then sustain a pre specified power flow from bus m to bus n, and control voltage at bus n.

Based on the predetermined values of power and voltage magnitude predicted to be imposed by the dynaflow, power flow is analysed. Parameters P, Q, | V | and δ on buses m and n are calculated on the basis of the power-flow solution [24, 25]. It is also possible to determine the internal control parameters of the dynaflow (i.e., k and $k_C X_C$) from Eq. (19). The complex power at bus m,

$$S_m = V_m I_m^* \tag{18}$$

Substituting for I_m from Eq. (12) in Eq. (18), it is deduced as

$$S_m = \frac{-(1+k^2)}{jX_{mn}}|V_m|^2 + \frac{(1+jk)}{jX_{mn}}V_m V_n^* \tag{19}$$

ISSN: 1992-8645 www.jatit.org E-ISSN: 1817-3195

Similarly, for S_n it is deduced as

$$S_n = \frac{-(1-jk)}{jX_{mn}} V_n V_m^* - \frac{X_{mn}}{jX_{mn}} |V_n|^2 \quad (20)$$

Detailed modeling of incorporating Dynaflow controller in conventional Newton – Raphson power flow is given in section 3.1.

3.1 Load Flow Modeling of Dynaflow Controller

The dynaflow should be changed in order to integrate the dynaflow into power flow equations using the systemic method. In this way, dynaflow equations can be written more easily in the power flow equations format. Fig. 4 shows this new model (extracted from Fig. 3). As illustrated by Fig. 4, the dynaflow model is transformed into a new model consisting only of a single series and a parallel branch. The series branch impedance is given in Eq. (21).

$$Z_{mn} = R_{mn} + jX_{mn} \quad (21)$$

So for the line between busses m and n from Eq. (9) can be written as

$$X_{mn} = k^2 X_E + X_B - k_C X_C + X_{LINE} \quad (22)$$

and $R_{mn} = Rl_{ine}$

Therefore, series branch admittance is as given as

$$Y_{TS} = Y_{mn} = 1/Z_{mn} = G_{TS} + jB_{TS} \quad (23)$$

Similarly parallel branch admittance from Eq. (16) can be written as

$$Y_{PS} = 1/Z_{PS} = G_{PS} + jB_{PS} \quad (24)$$

Where, $Z_{PS} = R_V + jX_P$

Parallel PST branches in Fig. 3 can be transformed into their thevenin equivalent, and parallel branches may be replaced by YPS admittance and EPS voltage sources, as shown in Fig. 4, following calculation of a thevenin parameter [26].

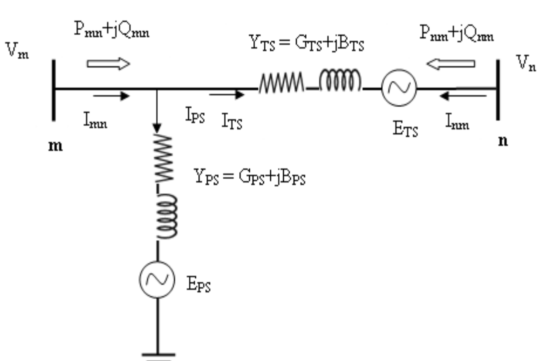

Fig. 4. New Circuit Model Of Dynaflow Device

The power flow equations for the generic bus (bus m) of the non-dynaflow power system is given in Eq. (25) & Eq. (26)

$$P_m = \sum |V_m||V_n||Y_{mn}| \cos(\delta_m - \delta_n - \theta_{mn}) \quad (25)$$

$$Q_m = \sum |V_m||V_n||Y_{mn}| \sin(\delta_m - \delta_n - \theta_{mn}) \quad (26)$$

Where

$|V_m| \angle \delta_m$ denotes the voltage & phase angle of bus m and $|Y_{mn}| \angle \theta_{mn}$ denotes elements of Ybus-matrix. Equations (25), (26) are iteratively solved using linearized Jacobian equation.

$$\begin{bmatrix} J_{11} & J_{12} \\ J_{21} & J_{22} \end{bmatrix} \begin{bmatrix} \Delta \delta \\ \Delta |V| \end{bmatrix} = \begin{bmatrix} \Delta P \\ \Delta Q \end{bmatrix} \quad (27)$$

Where the substrates of Jacobian in Eq. (27) are defined as:

$J_{11}=\partial P/\partial \delta$, $J_{12}=\partial P/\partial |V|$, $J_{21}=\partial Q/\partial \delta$, $J_{22}=\partial Q/\partial |V|$.

The flow equations for all Dynaflow buses in place are the same as those in the non-dynaflow system with the exception of the m and n buses written as as shown from Eq. (28) to (31).

$$P_m = P_{mn} + \sum |V_m||V_x||Y_{mx}| \cos(\delta_m - \delta_x - \theta_{mx}) \quad (28)$$

$$Q_m = Q_{mn} + \sum |V_m||V_x||Y_{mx}| \sin(\delta_m - \delta_x - \theta_{mx}) \quad (29)$$

$$P_n = P_{nm} + \sum |V_n||V_x||Y_{nx}| \cos(\delta_n - \delta_x - \theta_{nx}) \quad (30)$$

$$Q_n = Q_{nm} + \sum |V_n||V_x||Y_{nx}| \sin(\delta_n - \delta_x - \theta_{nx}) \quad (31)$$

For the system without Dynaflow, the quantitative terms in the above equations are the same. P_{mn}, Q_{mn} and vice-versa equations can be found in (32) to (35).

$$\begin{aligned} P_{mn} = {} & (G_{PS} + G_{TS})|V_m|^2 - \\ & |V_m||E_{PS}||Y_{PS}|\cos(\delta_m - \delta_{PS} - \theta_{PS}) \\ & + |V_m||E_{TS}||Y_{TS}|\cos(\delta_m - \delta_{TS} - \theta_{TS}) - \\ & |V_m||V_n||Y_{TS}|\cos(\delta_m - \delta_n - \theta_{TS}) \end{aligned} \quad (32)$$

$$Q_{mn} = (B_{PS} + B_{TS})|V_m|^2 - |V_m||E_{PS}||Y_{PS}|\sin(\delta_m - \delta_{PS} - \theta_{PS}) + |V_m||E_{TS}||Y_{TS}|\sin(\delta_m - \delta_{TS} - \theta_{TS}) - |V_m||V_n||Y_{TS}|\cos(\delta_m - \delta_n - \theta_{TS}) \quad (33)$$

$$P_{nm} = (G_{PS} + G_{TS})|V_n|^2 - |V_n||E_{PS}||Y_{PS}|\cos(\delta_n - \delta_{PS} - \theta_{PS}) + |V_n||E_{TS}||Y_{TS}|\cos(\delta_n - \delta_{TS} - \theta_{TS}) - |V_n||V_m||Y_{TS}|\cos(\delta_n - \delta_m - \theta_{TS}) \quad (34)$$

$$Q_{nm} = (B_{PS} + B_{TS})|V_n|^2 - |V_n||E_{PS}||Y_{PS}|\sin(\delta_n - \delta_{PS} - \theta_{PS}) + |V_n||E_{TS}||Y_{TS}|\sin(\delta_m - \delta_{TS} - \theta_{TS}) - |V_n||V_m||Y_{TS}|\cos(\delta_n - \delta_m - \theta_{TS}) \quad (35)$$

Four new variables ($|E_{PS}|$, δ_{PS}, $|E_{TS}|$, δ_{TS}) give rise to the energy flow problem by the voltage sources E_{PS} and E_{TS}. However |Vm| is known for its preset power flow values, so that one equation for voltages is solved. Three more equations are therefore needed to solve the problem of power flow. The equation of P_{mn} and Q_{mn} with its pre-specific target value would be two of these equations. Third equation is achieved by not exchanging real and reactive power with the system with the ideal dynaflow PST transformers. It is therefore possible to write as in Eq. (36).

$$P_{TCPST} = \text{real}\,[V_P.I_{mn}^*] - \text{real}\,[V_E.I_E^*] = 0 \quad (36)$$

These four equations must therefore be taken into consideration in order to implement Dynaflow in the conventional Newton-Raphson power flow algorithm.

3.2 Modifications in Jacobian elements of Dynaflow device

The Jacobian equation is extended and modified (37) to accommodate the added (32 to 36) equations and modified ones to solve the Dynaflow problem in order to resolve the power flow issue (38 to 61). As shown in Eq. (37), the original Jacobian matrix (yellow color filled in) contains three rows and three columns, although the added elements are mentioned in those rows and columns. The elements that need to be modified of the original Jacobian matrix are written in yellow cells. The original Jacobian matrix should contain 14 elements and add 31 elements as specified in Eq. (37).

Where the sub Jacobian matrices in Eq. (37) (yellow color filled in) are defined from Eq. (A.1-A.24) by using equation (28 to 35) in appendix

P_m/δ_m P_n/δ_m	P_m/δ_n P_n/δ_n	P_m/E_{PS} $P_n/\|V_n\|$	$P_m/\|V_n\|$	P_m/δ_{PS}	P_m/δ_{TS} P_n/δ_{TS}	$P_m/\|E_{TS}\|$ $P_n/\|E_{TS}\|$		$\Delta\delta$		ΔP
Q_m/δ_m Q_n/δ_m	Q_m/δ_n Q_n/δ_n	Q_m/E_{PS} $Q_n/\|V_n\|$	$Q_m/\|V_n\|$	Q_m/δ_{PS}	Q_m/δ_{TS} Q_n/δ_{TS}	$Q_m/\|E_{TS}\|$ $Q_n/\|E_{TS}\|$		ΔE_{PS} $\Delta\|V\|$		ΔQ
P_{PST}/δ_m	P_{PST}/δ_n	P_{PST}/E_{PS}	$P_{PST}/\|V_n\|$	P_{PST}/δ_{PS}	P_{PST}/δ_{TS}	$P_{PST}/\|E_{TS}\|$	×	$\Delta\delta_{PS}$	=	ΔP_{PST}
P_{mn}/δ_m	P_{mn}/δ_n	P_{mn}/E_{PS}	$P_{mn}/\|V_n\|$	P_{mn}/δ_{PS}	P_{mn}/δ_{TS}	$P_{mn}/\|E_{TS}\|$		$\Delta\delta_{TS}$		ΔP_{mn}
Q_{mn}/δ_m	Q_{mn}/δ_n	Q_{mn}/E_{PS}	$Q_{mn}/\|V_n\|$	Q_{mn}/δ_{PS}	Q_{mn}/δ_{TS}	$Q_{mn}/\|E_{TS}\|$		$\Delta\|E_{TS}\|$		ΔQ_{mn}

(37)

4. PROCEDURE FOR INCORPORATING DYNAFLOW CONTROLLER IN LOAD FLOW PROBLEM

Step 1: Read input data (bus, line and device data)
Step 2: Assume a flat voltage profile for all the buses except slack bus
Step 3: Iteration count k=0
Step 4: Find active and reactive power mismatches
Step 5: Find Jacobian matrix elements from load flow calculations
Step 6: Incorporate dynaflow device in the load flow and modify power mismatch and jacobian elements.
Step 7: Find voltage magnitudes and their angles by using newton raphson load flow equations.
Step 8: Use correction vector and update the solution
Step 9: Increase iteration count, k=k+1
Step 10: Stop the process it the mismatch was less than tolerance.

5. SIMULATION RESULTS

In this section, the proposed methodology is tested on IEEE 30 bus system. The dynaflow device is placed between buses 9 and 10 as it is identified as critical line i.e., nearer to generator buses and tap changing transformers. Line 9-10 is lightly loaded and it is close to the most severe contingency and congested lines. Hence in this work FACTS controllers are placed in the line connecting buses 9 and 10. In this paper, the results of test bus system are presented in two cases i.e. normal condition and contingency condition. In the first case, a comparison is made, without and with FACTS devices. In the second case, dynaflow controller is applied to alleviate overloads under selected set of network contingencies.

5.1 Normal Condition

In this case, the comparison of without FACTS and with considered FACTS devices such as TCPST, TSSC and Dynaflow is done to achieve coordinated control. The apparent power variations in six generator busses with FACTS devices are shown in Table 1. From Table 1, it can be observed that there is a considerable variation in the apparent flow of power with three FACTS devices.

FACTS, power flows can be controlled flexibly by the FACTS controller. Moreover, simulations show that the dynaflow controller provides independent control of active and reactive power transmissions. From the practical application aspect, the maximum value of the injected series voltage is due to the power rating of the dynaflow controller.

Table 1 Apparent Power (In P.U.) Of Generator Buses

Generator Number	Without FACTS	With TCPST	With TSSC	With Dynaflow controller
Generator 1	1.7723-j0.0778	1.7599-j0.2	1.746-j0.1837	1.7398-j0.2
Generator 2	0.4814+j0.3156	0.488+j0.2686	0.4839+j0.2214	0.4859+j0.1812
Generator 3	0.2147+j0.0647	0.2088+j0.3205	0.2205+j0.404	0.2249+j0.338
Generator 4	0.1214-j0.3189	0.1222-j0.1	0.1265-j0.1	0.125-j0.1
Generator 5	0.2138+j0.1123	0.2136+j0.2993	0.2141+0.2944	0.2145+j0.3117
Generator 6	0.12+j0.0781	0.12+j0.1475	0.12+j0.0009	0.12+j0.1404

The variations of the generator bus voltage are shown in Figure 5, and in Figure 6, the variations of the load bus voltage are shown. It is noted that with FACTS controllers the voltage is well maintained in load buses.

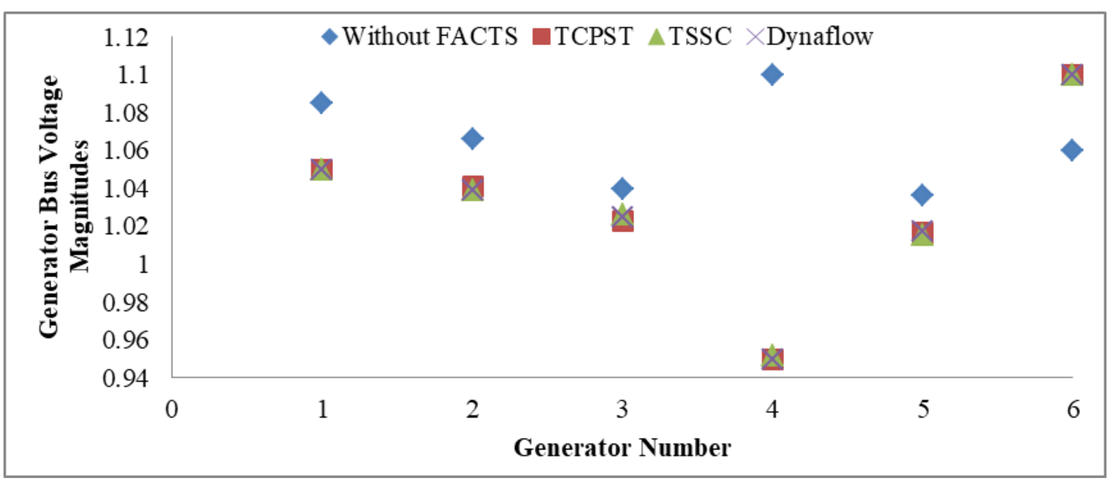

Fig. 5. Variation Of Generation Bus Voltage Magnitudes

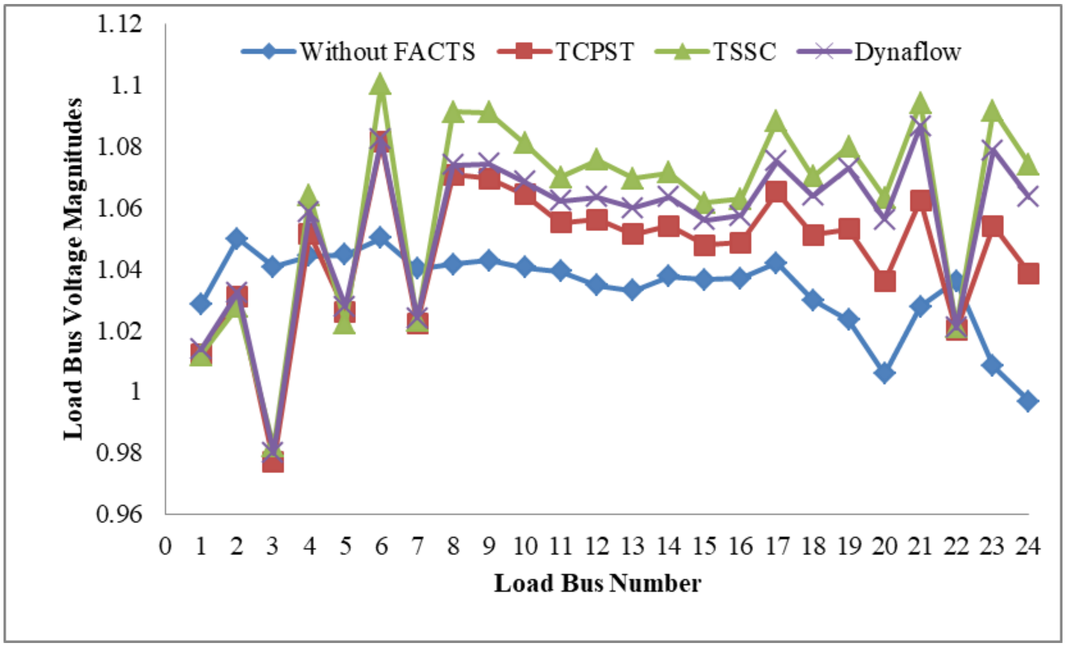

Fig. 6. Variation Of Load Bus Voltage Magnitudes

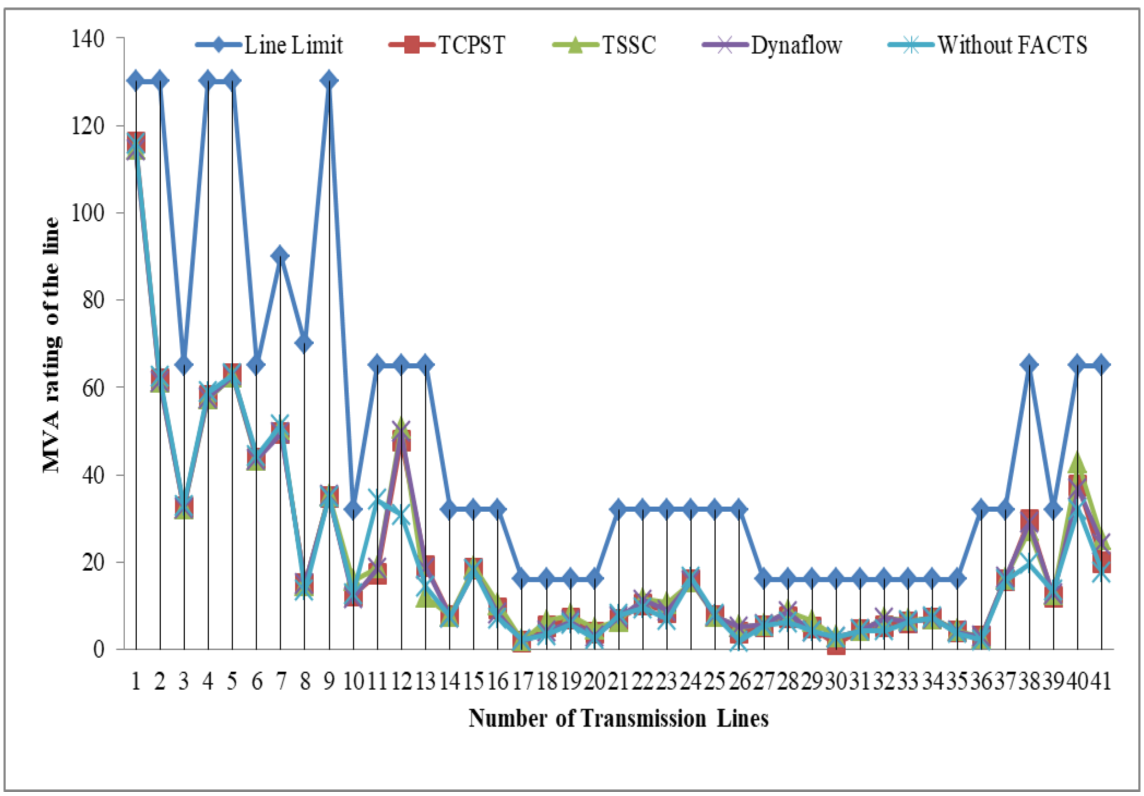

Fig. 7. Power Flow Variation In The Transmission Lines

ISSN: 1992-8645 www.jatit.org E-ISSN: 1817-3195

The change in power flow for normal load is shown in Figure 7 in the respective lines. This figure shows that the apparent power flow in lines connected to the device buses is significantly different.

5.2. Contingency Condition

The variation of the power flows in respective generator buses for the line connecting buses 2 and 5 contingency case is shown in Table 2. This table shows that the apparent flow of power in the buses attached to the generators is considerably different. The maximum variations in power flow are indicated.

Table 2 Apparent Power (In P.U.) Of Generator Buses Under 2-5 Contingency Condition

Generator Number	Without Dynaflow controller	With Dynaflow controller
Generator 1	1.8611-j0.0607	1.6350-j0.2
Generator 2	0.4823-j0.119	0.4316+j0.3418
Generator 3	0.2051+j0.0082	0.35+j0.3507
Generator 4	0.1236+j0.3272	0.1002-j0.0762
Generator 5	0.2142+j0.3781	0.2857+j0.324
Generator 6	0.12+j0.0854	0.1586+j0.3649

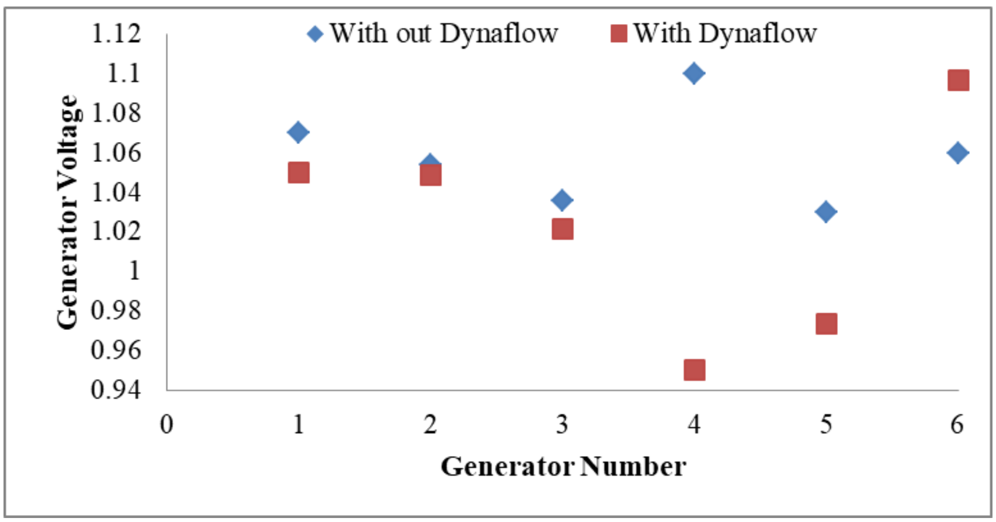

Fig. 8. Variation Of Generation Bus Voltage Magnitudes Under Contingency 2-5

Figure 8 shows the variations in the magnitude of generator bus voltage and Figure 9 shows the variations in the magnitude of load bus voltage. It is observed that, due to the voltage injection of the series controllers, maximum variation is observed on buses 3 and 7. Power flow variations in the transmission lines under contingency condition are shown in Figure 10. Lines 5 and 7 are overloaded with contingency of line connecting buses 2 and 5. Overload in the lines is relieved with dynaflow controller.

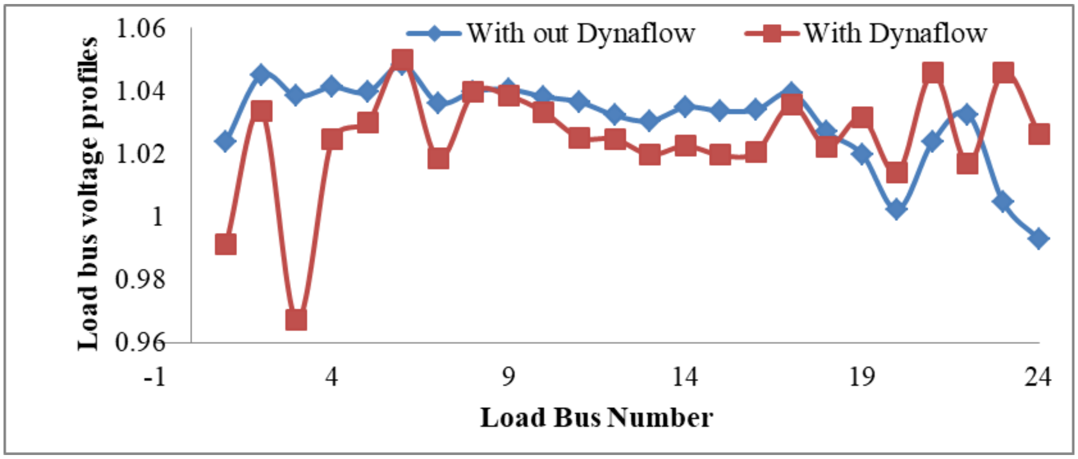

Fig. 9. Variation Of Load Bus Voltage Magnitudes Under Contingency 2-5

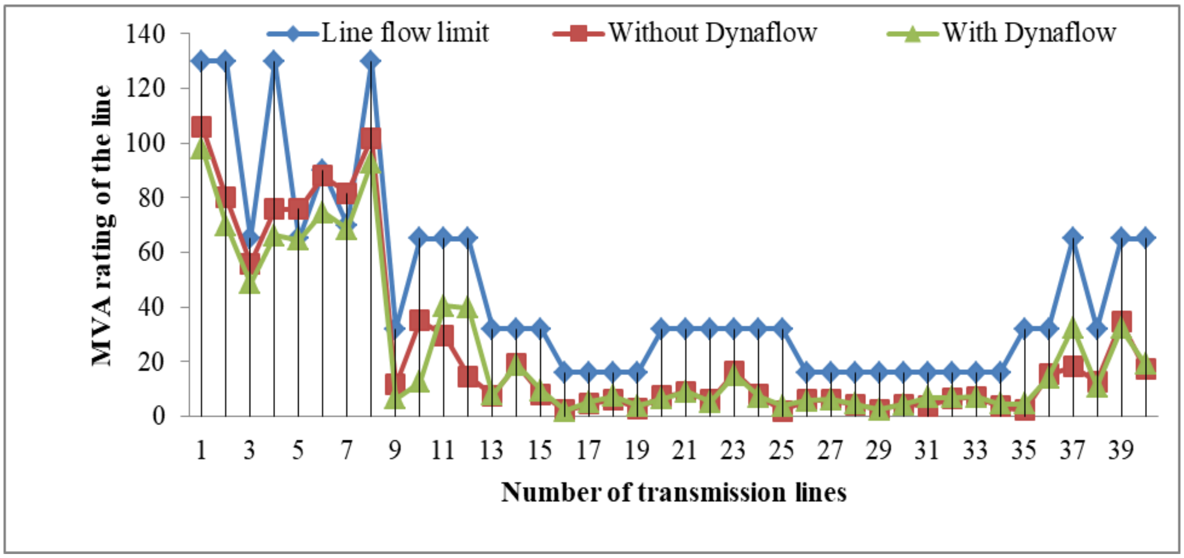

Fig.10. Power Flow Variation In The Transmission Lines

6. CONCLUSION

This paper presents a stable state mathematical model for the dynaflow controller. It can improve power flows in the transmission lines while keeping voltages at a stable value, the most important feature of the model. The algorithm of the Newton Raphson load flow can be kept intact by traditional techniques. As a consequence, the user-defined modelling techniques can directly use conventional techniques and even commercial power system analysis software.

Simulation studies show that a dynaflow controller can handle active and reactive power flow control in the transmission lines flexibly and independently. The result obtained from the bus test system IEEE-30 confirms that if proper control is provided, a device's effect is significant on system voltages and power flows.

REFRENCES:

[1] A. Edris, FACTS technology development: an update, IEEE Power Engineering Review, 20(3), (2000) 4-9. doi: 10.1109/39.825623.

[2] C. Lu, C. Hsu and C. Juang, Coordinated Control of Flexible AC Transmission System Devices Using an Evolutionary Fuzzy Lead-Lag Controller With Advanced Continuous Ant Colony Optimization,IEEE Transactions on Power Systems, 28(1), (2013) 385-392, doi: 10.1109/TPWRS.2012.2206410.

[3] Li-Jun Cai and I. Erlich, Simultaneous coordinated tuning of PSS and FACTS damping controllers in large power systems, IEEE Transactions on Power Systems, 20(1),(2005) 294-300, doi: 10.1109/TPWRS.2004.841177.

[4] H. F. Wang and F. J. Swift, A unified model for the analysis of FACTS devices in damping power system oscillations. I. Single-machine infinite-bus power systems, IEEE Transactions on Power Delivery, 12(2), (1997) 941-946,doi: 10.1109/61.584417.

[5] S. Y. Ge and T. S. Chung, "Optimal active power flow incorporating power flow control needs in flexible AC transmission systems," in IEEE Transactions on Power Systems, vol. 14, no. 2, pp. 738-744, May 1999, doi: 10.1109/59.761906.

[6] A. Mostafa, M. Ebeed, S. Kamel and M. A. Abdel-Moamen, "Optimal Power Flow Solution Using Levy Spiral Flight Equilibrium Optimizer With Incorporating CUPFC," in IEEE Access, vol. 9, pp. 69985-69998, 2021, doi: 10.1109/ACCESS.2021.3078115.

[7] N. H. Khan, Y. Wang, D. Tian, R. Jamal, S. Kamel and M. Ebeed, "Optimal Siting and Sizing of SSSC Using Modified Salp Swarm Algorithm Considering Optimal Reactive Power Dispatch Problem," in IEEE Access, vol. 9, pp. 49249-49266, 2021, doi: 10.1109/ACCESS.2021.3061503.

[8] H. Huang, L. Zhang, O. Oghorada and M. Mao, "Analysis and Control of a Modular Multilevel Cascaded Converter-Based Unified Power Flow Controller," in IEEE Transactions on Industry Applications, vol. 57, no. 3, pp. 3202-3213, May-June 2021, doi: 10.1109/TIA.2020.3029546.

[9] S. Dilshad, N. Abas, H. Farooq, A. R. Kalair and A. A. Memon, "NeuroFuzzy Wavelet Based Auxiliary Damping Controls for STATCOM," in IEEE Access, vol. 8, pp. 200367-200382, 2020, doi: 10.1109/ACCESS.2020.3031934.

[10] Y. Lei et al., "Comparison of UPFC, SVC and STATCOM in Improving Commutation Failure Immunity of LCC-HVDC Systems," in IEEE Access, vol. 8, pp. 135298-135307, 2020, doi: 10.1109/ACCESS.2020.3011113.

[11] I. Papic, P. Zunko, D. Povh and M. Weinhold, Basic control of unified power flow controller, IEEE Transactions on Power Systems, 12(4), (1997) 1734-1739, doi: 10.1109/59.627884.

[12] Qurratul Ain, Emad Jamil, Salman Hameed & Kumail Hasan Naqvi, Effects of SSSC and TCSC for enhancement of power system stability under different fault disturbances, Australian Journal of Electrical and Electronics Engineering, 17(1), (2020) 56-64, DOI: 10.1080/1448837X.2020.1752095

[13] Mohamed Ebeed, Salah Kamel, Francisco Jurado, Determination of IPFC operating constraints in power flow analysis, International Journal of Electrical Power & Energy Systems, 81 (2016), 299-307, https://doi.org/10.1016/j.ijepes.2016.02.044.

[14] Linash Kunjumuhammed, Stefanie Kuenzel, Bbikash Pal, Chapter Eight - Modelling of flexible AC transmission system devices, Simulation of Power System with Renewables, Academic Press, 2020, 205-224, https://doi.org/10.1016/B978-0-12-811187-1.00008-1.

[15] José M. Cano, Md. Rejwanur R. Mojumdar, Joaquín G. Norniella, Gonzalo A. Orcajo. Phase shifting transformer model for direct approach power flow studies, Electrical Power and Energy Systems 91 (2017) 71–79

[16] Ahmet Mete Vural, Emile Njodzefon Wirsiy, Three-phase modular multilevel converter based unified power flow controller, Engineering Science and Technology, an International Journal 23(2), (2020) 299–306

[17] A.M. Hemeida et al. TCSC with auxiliary controls based voltage and reactive power controls on grid power system. Ain Shams Engineering Journal 11 (2020) 587–609

[18] Yasir Muhammad, Rahimdad Khan, Muhammad Asif Zahoor Raja, Farman Ullah, Naveed Ishtiaq Chaudhary, Yigang He, Solution of optimal reactive power dispatch with FACTS devices: A survey, Energy Reports 6 (2020) 2211–2229

[19] Samo Gasperic, Rafael Mihalic, The impact of serial controllable FACTS devices on voltage stability, Electrical Power and Energy Systems 64 (2015) 1040–1048

[20] I. Papic, Mathematical analysis of FACTS devices based on a voltage source converter Part 1: mathematical models, Electric Power Systems Research 56(2), (2000) 139–148

[21] R. Srinivasa Rao, V. Srinivasa Rao, A generalized approach for determination of optimal location and performance analysis of FACTs devices, Electrical Power and Energy Systems 73 (2015) 711–724

[22] Ghadir Radman, Reshma S Raje, Power flow model/calculation for power systems with multiple FACTS controllers, Electric

Power Systems Research 77 (12), (2007) 1521–1531

[23] A. AL Ahmad, R. Sirjani. Optimal placement and sizing of multi-type FACTS devices in power systems using metaheuristic optimisation techniques: An updated review Ain Shams Engineering Journal 11(3) (2020) 611–628

[24] Roya Ahmadi, Abdolreza Sheykholeslami, Ali Nabavi Niaki, Hamidreza.Ghaffari. Power Flow Control and Solutions with Dynamic Flow Controller. IEEE Electrical Power & Energy Conference. Vancouver, BC, Canada, 2008.

[25] S. Ali Nabavi Niaki, Reza Iravani, and Mojtaba Noroozian. Power-Flow Model and Steady-State Analysis of the Hybrid Flow Controller. IEEE Transactions on Power Delivery, 23(4), (2008) 2330-2338.

[26] Ragaleela Dalapati Rao, Sivanagaraju Sirigiri, A novel particle movement bee colony algorithm with Dynaflow controller for line loadability enhancement, Engineering Science and Technology, an International Journal, 23(4), (2020),840-850.

Appendix

The sub Jacobian matrices in Eq. (37) (yellow color filled in) are defined as follows:

$$\frac{\partial P_m}{\partial \delta_{PS}} = -|V_m||E_{PS}||Y_{PS}|\sin(\delta_m - \delta_{PS} - \theta_{PS}) \quad (A.1)$$

$$\frac{\partial P_m}{\partial \delta_{TS}} = -|V_m||E_{TS}||Y_{TS}|\sin(\delta_m - \delta_{TS} - \theta_{TS}) \quad (A.2)$$

$$\frac{\partial P_n}{\partial \delta_{TS}} = -|V_n||E_{TS}||Y_{TS}|\sin(\delta_n - \delta_{TS} - \theta_{TS}) \quad (A.3)$$

$$\frac{\partial P_m}{\partial E_{TS}} = |V_m||Y_{TS}|\cos(\delta_m - \delta_{TS} - \theta_{TS}) \quad (A.4)$$

$$\frac{\partial P_n}{\partial E_{TS}} = -|V_n||Y_{TS}|\cos(\delta_n - \delta_{TS} - \theta_{TS}) \quad (A.5)$$

$$\frac{\partial Q_m}{\partial \delta_{PS}} = |V_m||E_{PS}||Y_{PS}|\cos(\delta_m - \delta_{PS} - \theta_{PS}) \quad (A.6)$$

$$\frac{\partial Q_m}{\partial \delta_{TS}} = -|V_m||E_{TS}||Y_{TS}|\cos(\delta_m - \delta_{TS} - \theta_{TS}) \quad (A.7)$$

$$\frac{\partial Q_n}{\partial \delta_{TS}} = |V_n||E_{TS}||Y_{TS}|\cos(\delta_n - \delta_{TS} - \theta_{TS}) \quad (A.8)$$

$$\frac{\partial Q_n}{\partial |E_{TS}|} = -|V_n||Y_{TS}|\sin(\delta_n - \delta_{TS} - \theta_{TS}) \quad (A.9)$$

$$\frac{\partial Q_m}{\partial |E_{TS}|} = |V_m||Y_{TS}|\sin(\delta_m - \delta_{TS} - \theta_{TS}) \quad (A.10)$$

$$\frac{\partial P_{mn}}{\partial \delta_m} = |V_m||E_{PS}||Y_{PS}|\sin(\delta_m - \delta_{PS} - \theta_{PS}) - |V_m||E_{TS}||Y_{TS}|\sin(\delta_m - \delta_{TS} - \theta_{TS}) + |V_m||V_n||Y_{TS}|\sin(\delta_m - \delta_n - \theta_{TS}) \quad (A.11)$$

$$\frac{\partial P_{mn}}{\partial \delta_n} = -|V_m||V_n||Y_{TS}|\sin(\delta_m - \delta_n - \theta_{TS}) \quad (A.12)$$

$$\frac{\partial P_{mn}}{\partial |E_{PS}|} = -|V_m||Y_{PS}|\cos(\delta_m - \delta_{PS} - \theta_{PS}) \quad (A.13)$$

$$\frac{\partial P_{mn}}{\partial V_n} = -|V_m||Y_{TS}|\cos(\delta_m - \delta_n - \theta_{TS}) \quad (A.14)$$

$$\frac{\partial P_{mn}}{\partial \delta_{PS}} = -|V_m||E_{PS}||Y_{PS}|\sin(\delta_m - \delta_{PS} - \theta_{PS}) \quad (A.15)$$

$$\frac{\partial P_{mn}}{\partial \delta_{TS}} = |V_m||E_{TS}||Y_{TS}|\sin(\delta_m - \delta_{TS} - \theta_{TS}) \quad (A.16)$$

$$\frac{\partial P_{mn}}{\partial |E_{TS}|} = |V_m||Y_{TS}|\cos(\delta_m - \delta_{TS} - \theta_{TS}) \quad (A.17)$$

$$\frac{\partial Q_{mn}}{\partial \delta_m} = -|V_m||E_{PS}||Y_{PS}|\cos(\delta_m - \delta_{PS} - \theta_{PS}) - |V_m||E_{TS}||Y_{TS}|\cos(\delta_m - \delta_{TS} - \theta_{TS}) - |V_m||V_n||Y_{TS}|\cos(\delta_m - \delta_n - \theta_{TS}) \quad (A.18)$$

$$\frac{\partial Q_{mn}}{\partial \delta_n} = |V_m||V_n||Y_{TS}|\cos(\delta_m - \delta_n - \theta_{TS}) \quad (A.19)$$

$$\frac{\partial Q_{mn}}{\partial |E_{PS}|} = -|V_m||Y_{PS}|\sin(\delta_m - \delta_{PS} - \theta_{PS}) \quad (A.20)$$

$$\frac{\partial Q_{mn}}{\partial |V_n|} = -|V_m||Y_{TS}|\sin(\delta_m - \delta_n - \theta_{TS}) \quad (A.21)$$

$$\frac{\partial Q_{mn}}{\partial \delta_{PS}} = |V_m||E_{PS}|\cos(\delta_m - \delta_{PS} - \theta_{PS}) \quad (A.22)$$

$$\frac{\partial Q_{mn}}{\partial \delta_{TS}} = -|V_m||E_{TS}||Y_{TS}|\cos(\delta_m - \delta_{TS} - \theta_{TS}) \quad (A.23)$$

$$\frac{\partial Q_{mn}}{\partial |E_{TS}|} = |V_m||Y_{TS}|\sin(\delta_m - \delta_{TS} - \theta_{TS}) \quad (A.24)$$